Ocean Engng, Vol. , No , pp. - , 1989.
Printed in Great Britain.

0029–8018/89 $3.00 + .00
Pergamon Press plc

HYDRODYNAMIC FORCES ON VERTICAL CYLINDERS AND THE LIGHTHILL CORRECTION

GRAHAM R. COOK and EMIL SIMIU
Center for Building Technology, National Bureau of Standards, Gaithersburg, MD 20899, U.S.A.

Abstract—In the keynote address to the 1979 Behaviour of Offshore Structures (BOSS) Conference, Sir James Lighthill pointed out the absence of a second-order term of potential origin from the Morison description of the hydrodynamic force on a vertical cylinder. This term, referred to as the Lighthill correction, is due to the nonlinear interaction between the flow velocity and its horizontal gradient. As noted by Lighthill, if this term is omitted, the estimated drag force in the Morison equation is equal in effect to the actual drag force *plus* the Lighthill correction.

Thus, it would appear that in cases where hydrodynamic damping plays an important role and should therefore be estimated as accurately as possible, corrections of the Lighthill type might have to be added to the Morison expression for the hydrodynamic force. (One such case is the dynamic amplification of wind-induced fluctuating motions of tension leg platforms.) In particular, it might be expected that the estimation of the damping force would be more strongly affected in situations involving low Keulegan–Carpenter numbers, and therefore relatively low damping forces.

It is thus of interest to examine the effect of the Lighthill correction quantitatively. In this work, the expression for the Lighthill correction was derived for finite water depths. Measurements obtained in periodic wave flow at the Naval Civil Engineering Laboratory and in random wave flow at the Delft Hydraulics Laboratory were subjected to an extensive analysis. The results of the analysis showed that for both the periodic and random wave conditions and addition of the Lighthill correction (1) did not improve the Morison equation significantly, and (2) had no significant effect on the estimation of the drag force, including the drag force corresponding to very low Keulegan–Carpenter numbers.

INTRODUCTION

WAVE FORCES on cylindrical elements are of considerable interest in the design of offshore facilities. Morison *et al.* (1950) proposed a simple equation expressing the total wave force as the sum of two components: an inertia force, due to the effects of irrotational (potential) flow, and a drag force, due to viscosity (skin friction and flow separation) effects. The equation is calibrated with two empirical coefficients which are referred to as the inertia and drag coefficient and are functions of the flow conditions.

The Morison equation has been criticized as oversimplifying the fluid mechanics of the loading but an alternative rigorous approach has not been developed to date. There appears to be a consensus that, to represent the fluid mechanics more closely, it is better to add correction terms to the Morison equation rather than devise a completely new relationship (Keulegan and Carpenter, 1958; Lighthill, 1979; Sarpkaya, 1981; Cook, 1987). The corrections of Keulegan, Carpenter and Sarpkaya are aimed essentially at accounting for vorticity effects. The topic of this paper, the Lighthill correction, is a correction associated with irrotational (potential) flow effects.

In his keynote address to the 1979 Conference on the Behaviour of Offshore Structures (BOSS) Sir James Lighthill showed that the force associated with the irrotational flow includes, in addition to the linear inertia term of the Morison equation, a nonlinear effect of potential origin due to the extensional motion (that is, the horizontal gradient of the in-line component of the flow velocity). Lighthill also noted that if the total force on a cylinder is expressed as the sum of the two Morison equation terms only, then the Lighthill force, which is due to potential flow effects, is automatically incorporated into the nonlinear drag term. This drag term is purportedly due solely to viscosity effects. Therefore, the Morison equation leads to an erroneous estimation of the force due to viscosity. The degree to which the error is significant depends upon the ratio between the Lighthill force and the actual Morison component associated with viscosity effects. This latter component is responsible for the bulk of damping that controls the dynamic response of compliant offshore structures to fluctuating wind (Simiu and Leigh, 1983; Cook *et al.*, 1986). The question of the extent to which corrections of the Lighthill type might affect the estimation of this component is therefore of significant practical interest in this context.

The primary objective of this paper is to investigate the significance of the Lighthill correction in quantitative terms. Two sets of data were used for the purpose of investigating the quantitative significance of the Lighthill correction. The first set was provided by the Naval Civil Engineering Laboratory (NCEL), and consisted of periodic flow force and flow measurements obtained in a wave tank (see Hudspeth and Nath (1985) for details). The second set was provided by the Delft Hydraulics Laboratory (DHL) and consisted of force and flow measurements obtained in a wave tank under random wave flow conditions (see Bearman *et al.* (1985a) for details).

THE MORISON EQUATION AND THE LIGHTHILL CORRECTION

The Morison equation (Morison *et al.*, 1950) is widely used in ocean engineering as an expression for wave-induced forces on structural members. For the case of a circular cylinder of diameter D, the Morison equation is usually expressed as

$$F = \frac{1}{4}\rho\pi D^2\, Cm \frac{du}{dt} + \frac{1}{2}\rho D\, Cd\, u\,|u| \qquad (1)$$

where F is the force per unit length, ρ is the fluid density, u is the undisturbed fluid velocity and Cd and Cm are the drag and inertia coefficients, respectively. With the widespread use of the Morison equation a great deal of work has been done on evaluating the appropriate values of the force coefficients. A review of this work is presented in Sarpkaya and Isaacson (1981).

As noted by Lighthill (1979) the fluid motion around a structure can be viewed as being due to (1) an irrotational flow that satisfies the boundary conditions, and (2) a vortex motion associated with any vorticity that has been shed (and satisfies zero boundary conditions, that is, zero fluid motion far from the body). It is the component due to the irrotational flow that Lighthill considers.

Lighthill derived two main second-order correction terms to the Morison equation. The corrections are due to the nonlinear interaction between a surface piercing cylinder and the irrotational flow field. The flow was assumed to consist of sinusoidal waves propagating in the positive x direction. The first correction term is a waterline force due to integration of the pressure between the still water level and the instantaneous free surface. If a body is totally submerged, as in the case of a horizontal cylinder or of nonsurface-piercing elements then this waterline force is not present. The second of

the correction terms is due to the horizontal gradient of the velocity (the extensional motion) and is given by the resultant of the dynamic pressure acting over the body's surface. Owing to the nature of the data being analysed in this paper we will consider the second correction only.

At any point in a fluid, if the velocity potential ϕ is known the fluid pressure at any point is determined by Bernoulli's equation

$$p = -p_s - \rho g z - \rho \frac{\partial \phi}{\partial t} - \frac{1}{2}\rho(\nabla\phi)^2 + C(t) \qquad (2)$$

where ρ is the fluid density, z is the distance from the still water level to the point being considered, g is the acceleration due to gravity, $C(t)$ is a function independent of the coordinates and p_s is the atmospheric pressure. Both ps and $C(t)$ may be taken equal to zero without loss of generality, see Stoker (1977).

Expanding the pressure p and the right-hand side of Equation (2) with respect to a perturbation parameter ϵ (ϵ is the wave steepness and equals ak, where a is the wave amplitude and k is the wavenumber) and equating powers of ϵ^2 we obtain the second order pressure as

$$p_2 = -\rho \frac{\partial \phi_2}{\partial t} - \frac{1}{2}\rho\,(\nabla\phi_1)^2. \qquad (3)$$

We seek the expression for ϕ_1 and ϕ_2 for the wave flow as modified by the presence of the cylinder. We first consider a potential flow with velocity u (in potential theory $u = \partial\phi/\partial x$) in the far field. The presence of a circular cylinder results in a flow field whose potential ϕ_d corresponds to a dipole (Milne-Thompson, 1960; p. 154), that is

$$\phi_d = u\left(r + \frac{b^2}{r}\right)\cos\theta \qquad (4)$$

where r is the radius to the point being considered, b is the cylinder radius and θ is the angle between the axis and the point being considered. If $\phi = \phi_d$ integration around the cylinder of the first term in Equation (3) yields the second order inertia force.

Setting ϕ equal to ϕ_d would be sufficient if the cylinder response was due to a fluctuating velocity only. However, in the case of a wave flow the in-line velocity has a nonzero horizontal gradient (extension) denoted by $E = \partial u/\partial x$. The extension can be expressed as a sum of a pure dilatation and a dilatationless strain (Lighthill, 1979). The cylinder responds to the variable extension because the cylinder itself impedes the local extensional motion of the fluid. This leads to a local compensating addition to the irrotational flow field, whose potential may be expressed as the sum of two terms:

(a) a monopole field associated with the pure dilatation to which there corresponds the potential, ϕ_m, equal to (Lighthill, 1979; p. 19).

$$\phi_m = \frac{E}{4}\left(r^2 - 2b^2 \ln\frac{r}{b}\right) \qquad (5)$$

where E is the extension and the other notations are the same as in Equation (4),

(b) a quadrupole field associated with the dilatationless strain to which there corresponds the potential, ϕ_q, equal to (Paterson, 1983; p. 217)

$$\phi_q = \frac{E}{4}\left(r^2 + \frac{b^4}{r^2}\right)\cos 2\theta \tag{6}$$

where the notation is the same as in Equations (4) and (5). Therefore, the total potential for the fluctuating extension is given as the sum of Equations (5) and (6), that is,

$$\phi_e = \frac{E}{4}\left(r^2 - 2b^2 \ln\frac{r}{b}\right) + \frac{E}{4}\left(r^2 + \frac{b^4}{r^2}\right)\cos 2\theta. \tag{7}$$

To include the response to the fluctuating extension in the dynamic pressure, the extension needs to be expanded in a power series

$$E = \epsilon E_1 + \epsilon^2 E_2 + \ldots \tag{8}$$

where $E_1 = \dfrac{\partial^2\phi_1}{\partial x^2}$ and $E_2 = \dfrac{\partial^2\phi_2}{\partial x^2}$.

The total extension potential, ϕ_e, expanded in the power series (8) gives

$$\phi_e = \epsilon\left\{\frac{E_1}{4}\left(r^2 - 2b^2\ln\frac{r}{b}\right) + \frac{E_1}{4}\left(r^2 + \frac{b^4}{r^2}\right)\cos 2\theta\right\} \tag{9}$$

$$+\ \epsilon^2\left\{\frac{E_2}{4}\left(r^2 - 2b^2\ln\frac{r}{b}\right) + \frac{E_2}{4}\left(r^2 + \frac{b^4}{r^2}\right)\cos\theta\right\}.$$

The basic fluctuating velocity potential, ϕ_d, can be expanded as

$$\phi_d = \epsilon u_1\left(r + \frac{b^2}{r}\right)\cos\theta + \epsilon^2 u_2\left(r + \frac{b^2}{r}\right)\cos\theta. \tag{10}$$

The total potential is equal to the sum of the dipole and extension potentials, that is $\phi = \phi_d + \phi_e$. Using polar coordinates and noting that $u_1 = \partial\phi_1/\partial x$ and $u_2 = \partial\phi_2/\partial x$ we obtain the horizontal and vertical velocities on the cylinder surface ($r = b$):

$$v_\theta = \frac{1}{r}\frac{\partial\phi}{\partial\theta} = \frac{1}{r}\frac{\partial}{\partial\theta}(\epsilon\,\phi_1 + \epsilon^2\,\phi_2) \tag{11}$$

$$= \epsilon\left(-E_1\, b\sin 2\theta - 2\frac{\partial\phi_1}{\partial x}\sin\theta\right) +$$

$$\epsilon^2\left(-E_2\, b\sin 2\theta - 2\frac{\partial\phi_2}{\partial x}\sin\theta\right)$$

and

$$v_z = \frac{\partial\phi}{\partial z} = \frac{\partial}{\partial z}(\epsilon\,\phi_1 + \epsilon^2\,\phi_2) \tag{12}$$

$$= \epsilon\left(\frac{\partial\phi_1}{\partial z} + 2\frac{\partial^2\phi_1}{\partial x\partial z}b\cos\theta + \frac{1}{4}\frac{\partial E_1}{\partial z}b^2 + \frac{1}{2}\frac{\partial E_1}{\partial z}b^2\cos 2\theta\right)$$

$$+\ \epsilon^2\left(\frac{\partial\phi_2}{\partial z} + 2\frac{\partial^2\phi_2}{\partial x\partial z}b\cos\theta + \frac{1}{4}\frac{\partial E_2}{\partial z}b^2 + \frac{1}{2}\frac{\partial E_2}{\partial z}b^2\cos 2\theta\right).$$

We can now calculate the total second order dynamic pressure, $p_{2d} = (1/2\rho(\nabla\phi_1)^2)$,

$$p_{2d} = -\frac{\rho}{2}\left\{E_1^2\, b^2\sin^2 2\theta + 4\frac{\partial\phi_1}{\partial x}E_1\, b\sin 2\theta\sin\theta\right.$$

$$+\ 4\left(\frac{\partial\phi_1}{\partial x}\right)^2\sin^2\theta + \left(\frac{\partial\phi_1}{\partial z}\right)^2 + 4\frac{\partial\phi_1}{\partial z}\frac{\partial^2\phi_1}{\partial x\partial z}b\cos\theta$$

$$+\ \frac{1}{2}\frac{\partial\phi_1}{\partial z}\frac{\partial E_1}{\partial z}b^2 + \frac{\partial\phi_1}{\partial z}\frac{\partial E_1}{\partial z}b^2\cos 2\theta + 4\left(\frac{\partial^2\phi_1}{\partial x\partial z}\right)^2 b^2\cos^2\theta$$

$$+\ \frac{\partial^2\phi_1}{\partial x\partial z}\frac{\partial E_1}{\partial z}b^3\cos\theta + 2\frac{\partial E_1}{\partial z}\frac{\partial^2\phi_1}{\partial x\partial z}b^3\cos\theta\cos 2\theta$$

$$+\ \frac{1}{16}\left(\frac{\partial E_1}{\partial z}\right)^2 b^4 + \frac{1}{4}\left(\frac{\partial E_1}{\partial z}\right)^2 b^4\cos 2\theta$$

$$\left.+\ \frac{1}{4}\left(\frac{\partial E_1}{\partial z}\right)^2 b^4\cos^2 2\theta\right\}. \tag{13}$$

The dynamic force around the cylinder is calculated as follows

$$F_{dy} = \int \frac{1}{2}\rho\,(\nabla\phi_1)^2\, n_x\, \mathrm{d}s$$

$$= \rho\pi b^2\, u_{1x}\, E_1 + 2\rho\pi b^2\, u_{1z}\frac{\partial u_{1z}}{\partial x} + 2\rho\pi b^4\frac{\partial u_{1z}}{\partial x}\frac{\partial E_1}{\partial z} \tag{14}$$

where the integral is taken over the wetted perimeter, n_x is the x component of the unit normal pointing toward the body, $u_{1x} = \partial\phi_1/\partial x$ is the first order velocity in the x direction, $E_1 = \partial^2\phi_1/\partial x^2$ is the first order extension in the x direction, $u_{1z} = \partial\phi_1/\partial z$ is the first order velocity in the z direction and the other notations are as given previously. The total force on the section being considered is

$$F_{2d} = \int F_{dy}\,\mathrm{d}z \tag{15}$$

where the integral is taken between the top and bottom of the submerged element being considered. For slender cylinders the last term in Equation (14) turns out to be insignificant compared to the first two. For $kh > \pi$, using Stokes first order theory we obtain Lighthill's results for deep water waves, that is

$$u_{1x}\, E_1 \simeq -\, u_{1z}\frac{\partial u_{1z}}{\partial x} \tag{16}$$

and

$$F_{dy} = -\,\rho\pi b^2\, u_{1x}\, E_1\,. \tag{17}$$

The total force acting on an elemental section of a circular cylinder is now equal to the two Morison equation terms plus the second order Lighthill correction (Equation (14)). According to Lighthill the analysis for his correction is equally applicable in random wave fields. If the analysis is to be performed in the time domain then the velocity is simply the local fluctuating velocity and the extension is the local fluctuating extension in the wave field.

The extension E and the spatial derivative of the vertical velocity u_z and of E, which are needed in Equation (14) were not measured, since such measurements cannot be carried out in practice. The quantities, E_1, $\partial u_{1z}/\partial x$ and $\partial E_1/\partial z$ were estimated from measured flow properties as follows. For the periodic flow use was made of relations based on Stokes second order wave theory (Cook, 1987). For the random flow the measured records were decomposed into Fourier series and the requisite quantities were obtained by differentiation of the terms of the series so obtained.

ANALYSIS OF THE PERIODIC DATA

This section deals with the results of the analysis of the periodic data based on the Morison equation alone and then considers the effect of including the Lighthill correction. The data obtained from NCEL included the wave profile, in-line force and velocity measurements for a reasonable range of wave heights and wave periods.

Least squares analyses were performed to obtain the time invariant coefficients *Cd* and *Cm* based on the Morison equation. Figure 1 plots the drag coefficients for each individual wave, showing their variation with Keulegan–Carpenter number ($KC = u\,T/D$ and is the ratio of the measure of the path length of a fluid particle during a wave period T, to the body diameter D). The drag coefficients show a large variability at low KC numbers. This may be expected because the drag term is small relative to the inertia term and instabilities occur in its calculation. Note that above $KC \approx 4$ the drag term is more significant and shows little variation with increasing KC numbers. It is noted that the dependence of the drag coefficient on KC is similar to that reported by Sarpkaya (1976).

Figure 2 plots the inertia coefficient against the KC number. It can be seen that at low KC numbers ($KC < 4$) the inertia coefficient is greater than the ideal potential

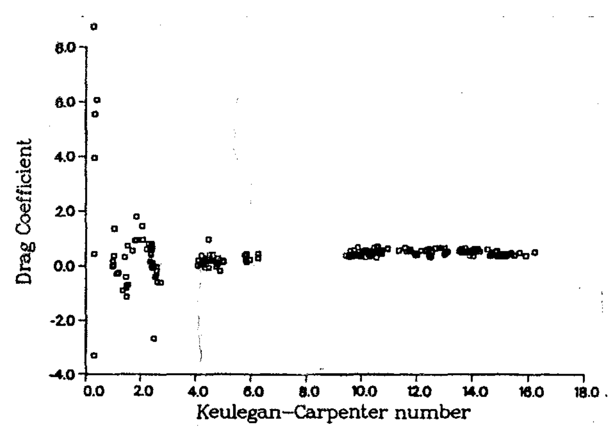

Fig. 1. Drag coefficient vs Keulegan–Carpenter number.

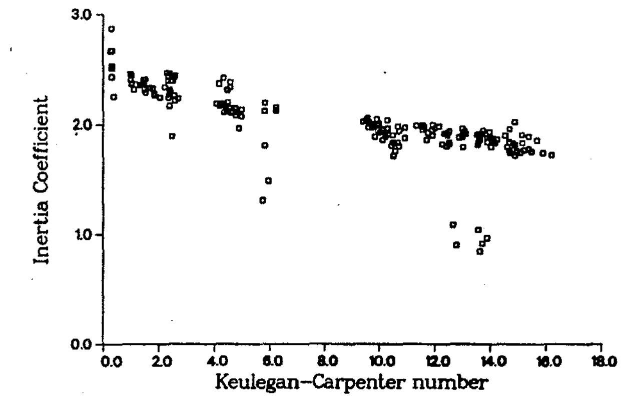

Fig. 2. Inertia coefficient vs Keulegan–Carpenter number.

flow value of 2.0. This is in agreement with results obtained by Chakrabarti *et al.* (1976) and Chakrabarti (1980) who also reported values of *Cm* significantly greater than 2. Note that $Cm = 2$ if the effects of viscosity are neglected. Such effects are included in expressions for *Cm* given by Sarpkaya (1986) and Bearman *et al.* (1985b). However, these expressions are based on a linearization of the Navier–Stokes equations which is acceptable only if the frequencies of the wave motion are very high. This linearization is not applicable in the case of ocean or wave tank data.

Force time histories were calculated both for the full records and for each individual wave of the full record. The forces were calculated by assuming the validity of the Morison equation with time invariant coefficients. Figures 3–6, based on the analysis of the full record, show measured and calculated force time histories for the lowest KC ($KC = 0.32$), as well as for $KC = 4.41$, $KC = 10.26$, and the highest KC ($KC = 15.31$), respectively. Also shown on these plots is the force residue, that is, the difference between the measured and the calculated force histories. In all figures pertaining to the periodic data, measured and calculated forces are represented by solid and interrupted lines respectively, and force residues are represented by dash–dot lines.

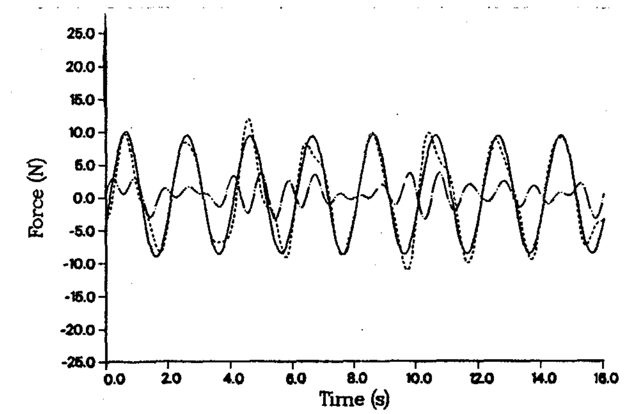

Fig. 3. Force time histories: measured (——); Morison equation (---); force residue (—·—); $KC = 0.32$.

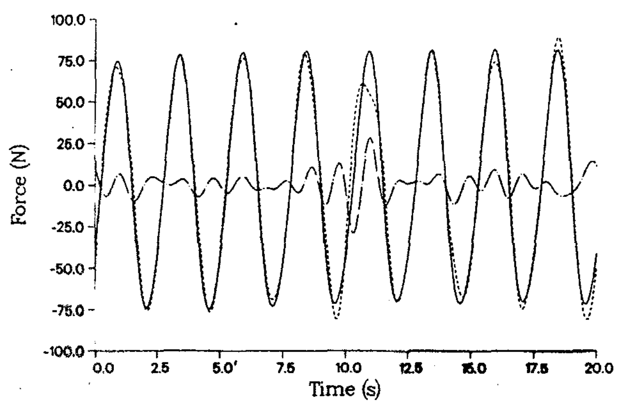

Fig. 4. Force time histories: measured (——); Morison equation (---); force residue (—·—·); $KC = 4.41$.

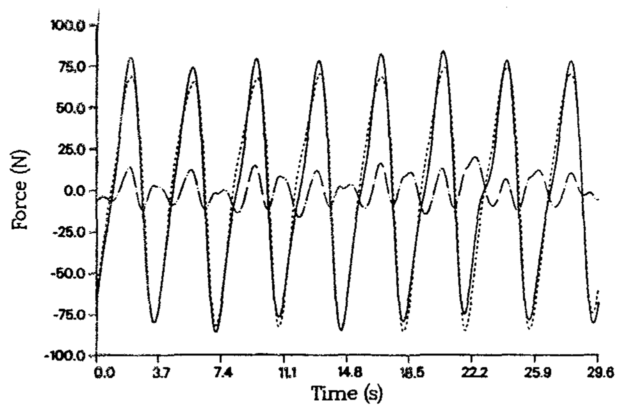

Fig. 5. Force time histories: measured (——); Morison equation (---); force residue (—·—·); $KC = 10.26$.

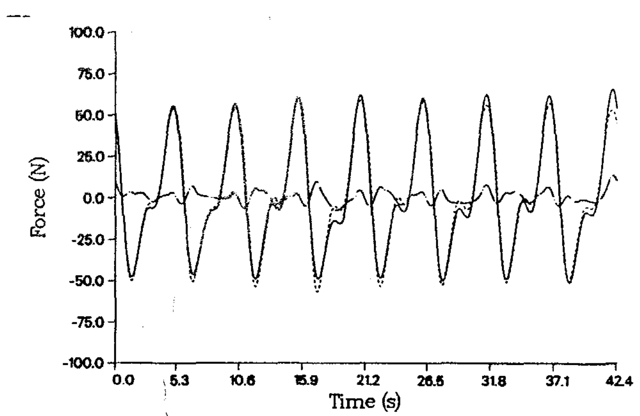

Fig. 6. Force time histories: measured (——); Morison equation (---); force residue (—·—·); $KC = 15.31$.

The dominant harmonic of the residue for all the force histories appears to be close to the second harmonic of the force. It is noted that the Lighthill correction term also has frequencies equal to twice the fundamental frequency.

Results corresponding to typical individual waves from each of the runs plotted in Figs 3–6 are given in Figs 7–10. It was found that for all waves the dominant harmonic of the residue appears to be close to the second harmonic of the force.

A separate analysis was conducted by assuming the forces to be described by the Morison equation (with time invariant coefficients) corrected by the addition of the Lighthill term. Figures 11–14 plot the calculated forces for the full records. When Figs 11–14 are compared to Figs 3–6 it can be seen that the difference between the respective force residues is minimal. This can be seen more clearly in Fig. 15 where the r.m.s. errors for the Morison equation are compared with those for the Morison equation with the Lighthill correction.

We now consider the time histories for individual waves. Figures 16–19 show the measured force, the calculated force based on the Morison equation with the Lighthill

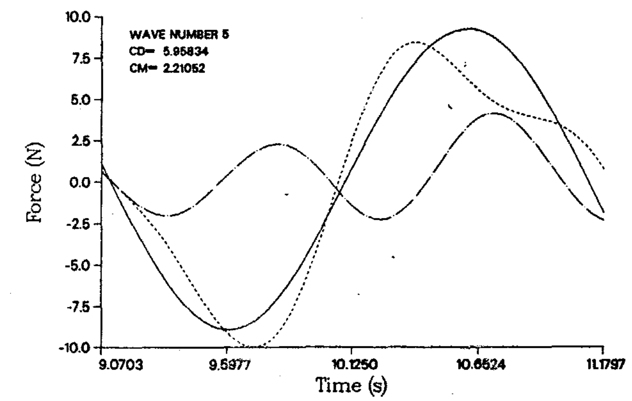

Fig. 7. Individual wave force time histories: measured (——); Morison equation (---); force residue (—·—·); $KC = 0.32$.

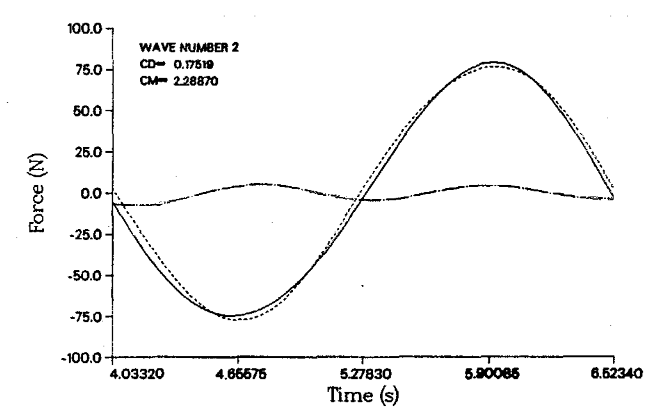

Fig. 8. Individual wave force time histories: measured (——); Morison equation (---); force residue (—·—·); $KC = 4.41$.

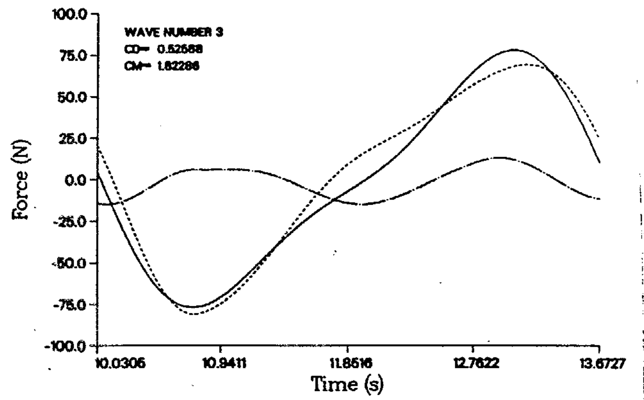

Fig. 9. Individual wave force time histories: measured (——); Morison equation (---); force residue (—·—); KC = 10.26.

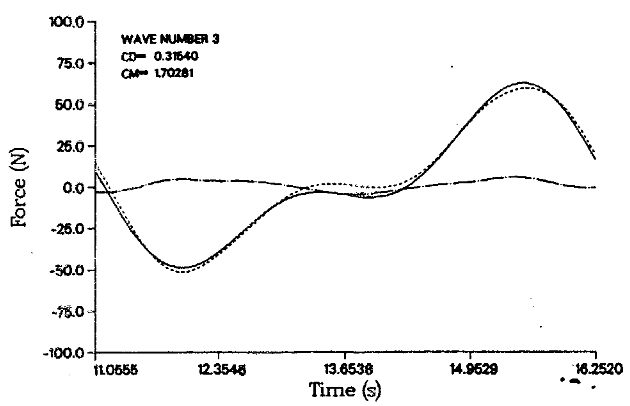

Fig. 10. Individual wave force time histories: measured (——); Morison equation (---); force residue (—·—); KC = 15.31.

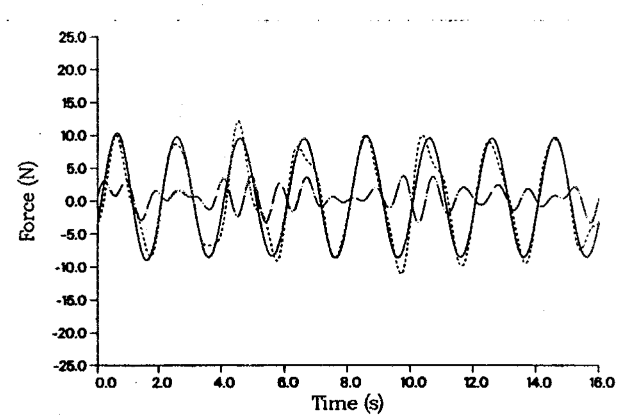

Fig. 11. Force time histories: measured (——); Morison equation with Lighthill correction (---); force residue (—·—); KC = 0.32.

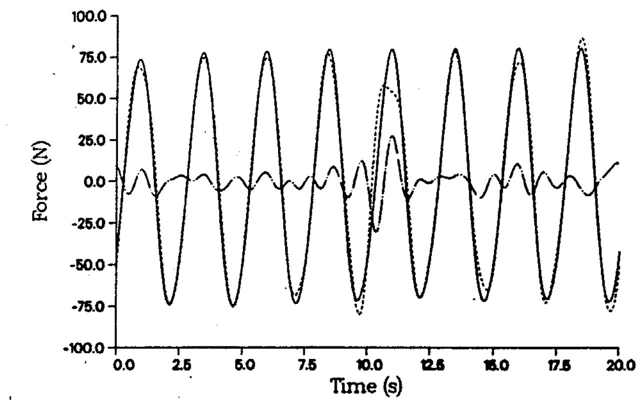

Fig. 12. Force time histories: measured (——); Morison equation with Lighthill correction (---); force residue (—·—); KC = 4.41.

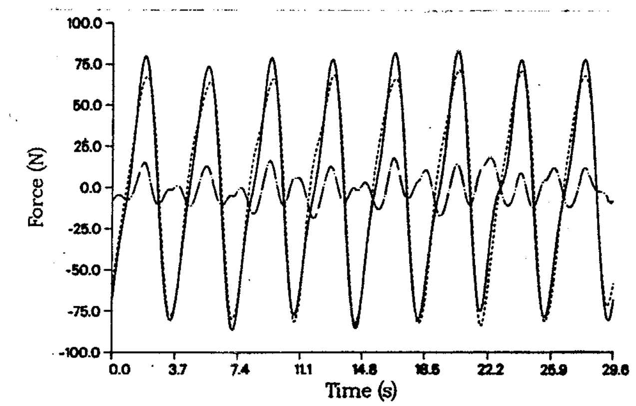

Fig. 13. Force time histories: measured (——); Morison equation with Lighthill correction (---); force residue (—·—); KC = 10.26.

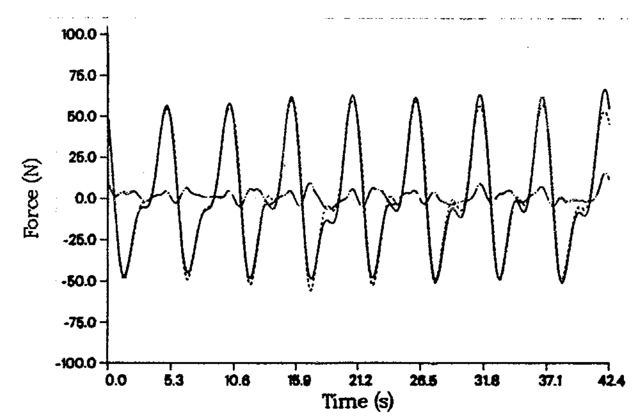

Fig. 14. Force time histories: measured (——); Morison equation with Lighthill correction (---); force residue (—·—); KC = 15.31.

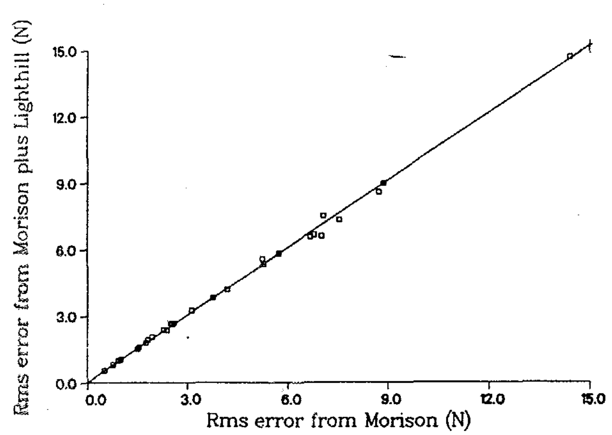

Fig. 15. R.m.s. errors for the time histories obtained by the Morison equation with the Lighthill correction vs the r.m.s. errors for the time histories obtained by the Morison equation.

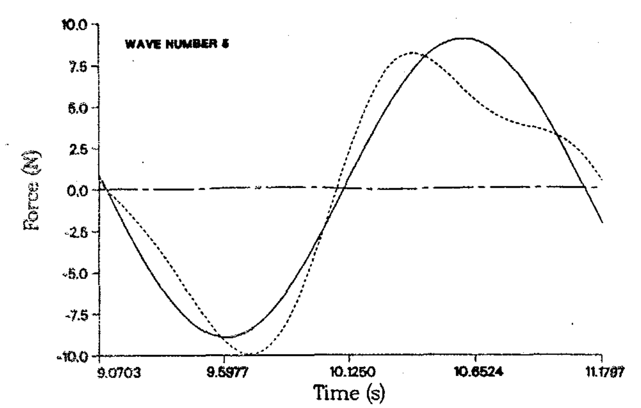

Fig. 16. Individual wave force time histories: measured (——); Morison equation with the Lighthill correction (---); Lighthill correction (— - —); KC = 0.32.

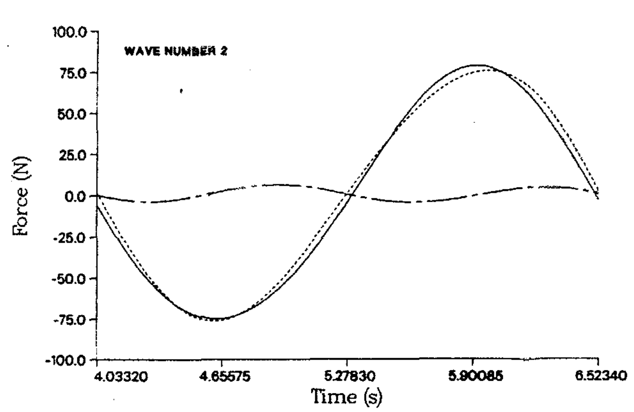

Fig. 17. Individual wave force time histories: measured (——); Morison equation with Lighthill correction (---); Lighthill correction (— - —); KC = 4.41.

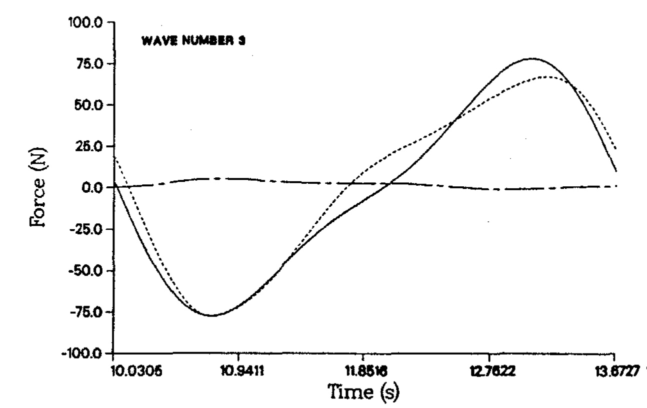

Fig. 18. Individual wave force time histories: measured (——); Morison equation with the Lighthill correction (---); Lighthill correction (— - —); KC = 10.26.

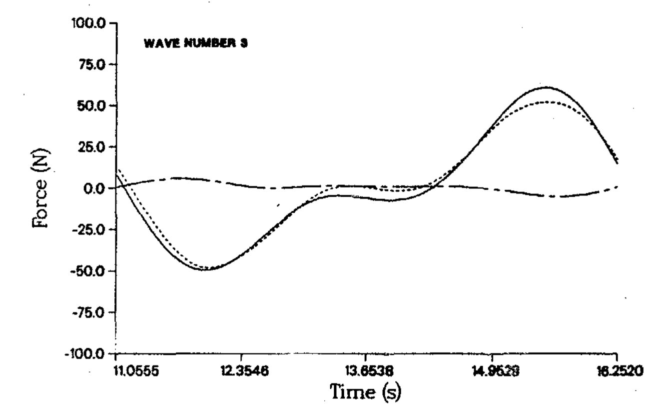

Fig. 19. Individual wave force time histories: measured (——); Morison equation with the Lighthill correction (---); Lighthill correction (— - —); KC = 15.31.

correction and the Lighthill correction itself. (In all figures the Lighthill correction is represented by long-dash–short-dash lines.) An overall assessment of the Lighthill correction can be made by comparing the r.m.s. error for the Morison equation with the Lighthill correction against the r.m.s. error for the Morison equation without correction. Figure 20 shows this comparison for each of the waves analysed. It can be seen that generally the modeling by the Morison equation is slightly better than the modeling by the Morison equation with the Lighthill correction. However, the differences are marginal.

Calculations were also performed to examine the effect of the Lighthill correction on the drag and inertia coefficients. The results can be seen in Figs 21 and 22 where the drag and inertia coefficients, respectively, are shown for the individual wave results. These two figures plot the force coefficients based on the Morison equation with the Lighthill correction (squares), and the force coefficients based on the Morison equation (triangles) superimposed. It can be seen that there is very little difference in the drag

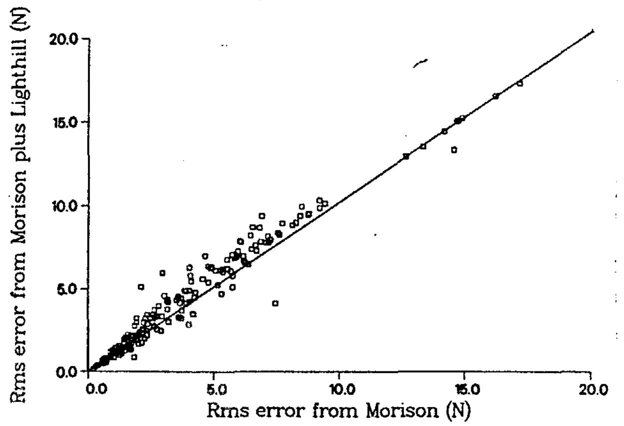

FIG. 20. Rms errors for the time histories obtained by the Morison equation with the Lighthill correction vs the r.m.s. errors for the time histories obtained by the Morison equation.

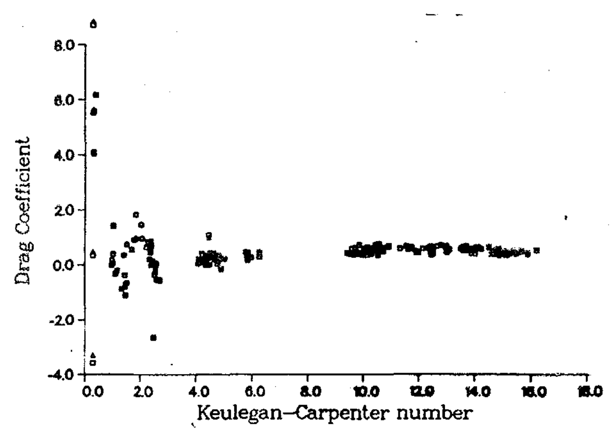

FIG. 21. Comparison of drag coefficients.

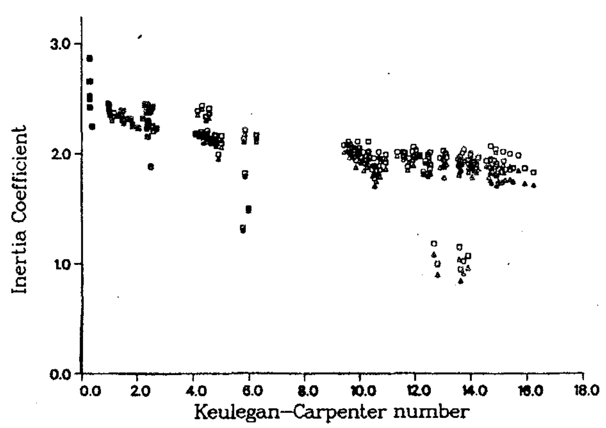

FIG. 22. Comparison of inertia coefficients.

coefficients over the whole range of KC numbers considered. For the inertia coefficients the largest error, although still small, occurs at the higher KC numbers. Hence, it can be concluded that for the NCEL data the addition of the Lighthill correction does not decrease the drag coefficient significantly.

ANALYSIS OF THE RANDOM DATA

The data obtained from DHL included the in-line force, the horizontal and vertical velocity, all measured at 2.5m (the lower level) and 3.5m (the upper level) above the bottom of the tank and wave elevations which were measured upstream and downstream of the cylinder.

The effective Keulegan–Carpenter numbers as defined by Bishop (1978) ($KC^* = (2\pi/0.866D)\sqrt{(u^4/a^2)}$ were u is the velocity, a is the acceleration and D is the cylinder diameter) where $KC^* = 5.75$ for the lower level and $KC^* = 6.0$ for the upper level. These low KC^* values indicate that the dominant part of the total Morison force is due to the inertia term. Since the Lighthill correction affects the inertia term, its effect may therefore be expected to be most significant in the low KC^* region.

Least squares analyses of the full time histories of the measured forces, velocities and accelerations were performed to estimate the drag and inertia coefficients in the Morison equation without a correction term. The values so obtained were $Cd = 0.2345$ and $Cm = 1.8295$ for the lower level and $Cd = 0.5393$ and $Cm = 2.0502$ for the upper level. Force spectra were then calculated using the Morison equation in which these coefficients and the measured velocity and acceleration were used. Figures 23 and 24 show, for the lower and upper levels, respectively, these calculated force spectra (dashed line) and the spectra of the measured forces (solid line). It is seen that the Morison equation with time invariant coefficients provides an excellent fit to the measured forces.

Least squares analyses were also performed to obtain the drag and inertia coefficients when the Lighthill correction term was included in the calculation of the forces. The coefficients obtained from the analyses were $Cd = 0.2341$, $Cm = 1.8343$ for the lower level and $Cd = 0.5403$, $Cm = 2.0587$ for the upper level. When these coefficients are

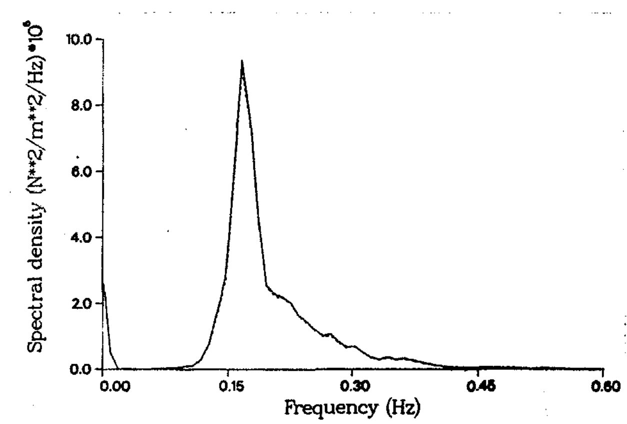

FIG. 23. Spectral density of Morison equation forces and measured forces.

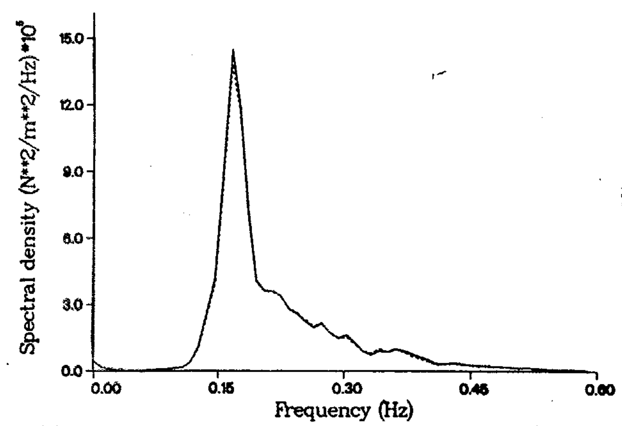

Fig. 24. Spectral density of Morison equation forces and measured forces.

compared to those obtained by using the Morison equation without correction it can be seen that the effect of the Lighthill term is minimal (of the order of 0.5% or less). That the Lighthill term has no significant contribution to the total force is also borne out by the measured force spectra (solid line) and the calculated force spectra (dashed line) shown in Figs 25 and 26 for the lower and upper levels, respectively. Indeed, it can be seen that the addition of the Lighthill correction does not change significantly the calculated spectra with respect to their values based on the Morison equation with no correction (see Figs 23 and 24).

It is concluded that the Morison equation provides an excellent model for the DHL measured forces, and that the inclusion of the Lighthill correction term makes no significant difference for both the force coefficients and the calculated force spectra.

CONCLUSIONS

The Morison equation with time invariant coefficients provides an excellent model for both the periodic and the random data analysed in this paper. The Lighthill

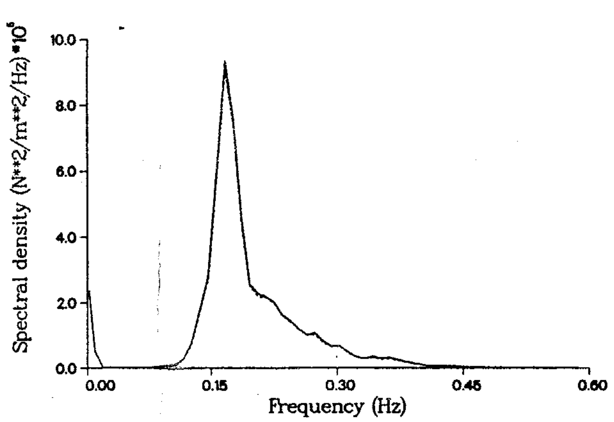

Fig. 25. Spectral density of Morison equation with Lighthill correction forces and measured forces.

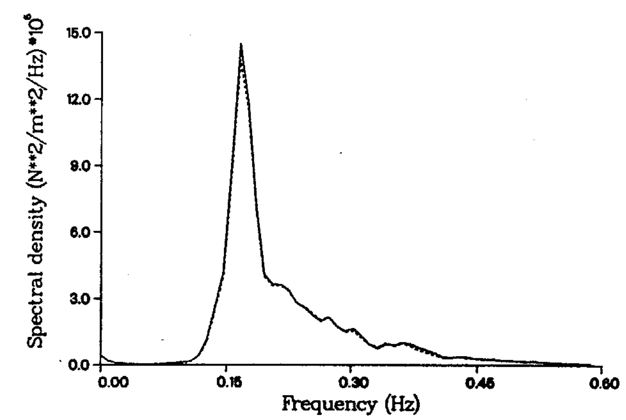

Fig. 26. Spectral density of Morison equation with Lighthill correction forces and measured forces.

correction did not improve the performance of the Morison equation and did not alter the drag coefficient to any significant extent.

Acknowledgements—Thanks are due to the following establishments or people: (i) Minerals Management Service, U.S. Department of the Interior, which provided partial support for this work. Mr Charles E. Smith served as Research Program Manager, (ii) The Delft Hydraulics Laboratory in the Netherlands which supplied the random data and (iii) The Naval Civil Engineering Laboratory at Port Hueneme, California which supplied the periodic data.

REFERENCES

Bearman, P. W., Chaplin, J. R., Graham, J. M. R., Kostense, J. K., Hall, P. F. and Klopman, G. 1985a. The loading on a cylinder in post-critical flow beneath periodic and random waves. Behaviour of Offshore Structures (BOSS '85), The Netherlands.

Bearman, P. W., Downie, M. J., Graham, J. M. R. and Obasaju, E. D. 1985b. Forces on cylinders in viscous oscillatory flow at low Keulegan–Carpenter numbers. *J. Fluid Mechanics* **154**, ●●●–●●●.

Bishop, J. R. 1978. The mean square value of wave force based on the Morison equation. National Maritime Institute Report NMI-R-40.

Chakrabarti, S. 1980. In-line forces on fixed vertical cylinders in waves. *J. WatWays, Port, Coastal Ocean Div. Am. Soc. civ. Engrs* **106** (WW2), ●●●–●●●.

Chakrabarti, S., Wolbert, A. and Tam, W. 1976. Wave forces on a vertical cylinder. *J. WatWays, Harbor Coastal Engng Am. Soc. civ. Engrs* **102** (WW2), ●●●–●●●.

Cook, G. R. 1987. The Lighthill correction to the Morison equation. Ph.D. dissertation submitted to the Johns Hopkins University, Baltimore.

Cook, G. R., Kumarasena, T. and Simiu, E. 1986. Amplification of wind effects on compliant platforms. Proceedings of a session at Structures Congress '86, ASCE.

Hudspeth, R. T. and Nath, J. H. 1985. High Reynolds number wave force investigation in a wave flume. Report No. CR 85.004, Naval Civil Engineering Laboratory, Port Hueneme, CA.

Keulegan, G. H. and Carpenter, L. H. 1958. Forces on cylinders and plates in an oscillatory fluid. *J. Res. natn. Bur. Standrds.* **60**(5), ●●●–●●●.

Lighthill, J. 1979. Waves and hydrodynamic loading. *Proc. 2nd Int. Conf. on the Behaviour of Offshore Structures BOSS '79, London,* Vol. 1.

Milne-Thomson, L. M. 1960. *Theoretical Hydrodynamics*, 4th edn. MacMillan, New York.

Morison, J. R., O'Brien, M. P., Johnson, J. W. and Schaaf, S. A. 1950. The forces exerted by surface waves on piles. *Petroleum Trans.* **189**, ●●●–●●●.

Paterson, A. R. 1983. *A First Course in Fluid Dynamics*. Cambridge University Press, Cambridge.

Sarpkaya, T. 1976. In-line and transverse forces on smooth and sand roughened cylinders in oscillatory flow at high Reynolds numbers. Report No. NPS-69SL76062, Naval Postgradduate School, Monterey, CA.

Sarpkaya, T. 1981. Morison equation and the wave forces on offshore structures. Report No. CR 82.008, Naval Civil Engineering Laboratory, Port Hueneme, CA.

Sarpkaya, T. 1986. Force on a circular cylinder in viscous oscillatory flow at low Keulegan–Carpenter numbers. *J. Fluid Mechanics* **165**, ●●●–●●●.

Sarpkaya, T. and Isaacson, M. 1981. *Mechanics of Wave Forces on Offshore Structures*. Van Nostrand Reinhold, New York.

Simiu, E. and Leigh, S. D. 1983. Turbulent wind effects on compliant platforms. NBS Building Science Series 151.

Stoker, J. J. 1957. *Water Waves*. Wiley Interscience, New York.